Optimal sensor set for decoding motor imagery from EEG

Dillen, Arnau; Ghaffari, Fakhreddine; Romain, Olivier; Vanderborght, Bram; Meeusen, Romain; Roelands, Bart; De Pauw, Kevin

Published in:
11th International IEEE EMBS Conference on Neural Engineering

DOI:
10.1109/NER52421.2023.10123875

Publication date:
2023

Optimal sensor set for decoding motor imagery from EEG

Arnau Dillen*†, Fakhreddine Ghaffari†, Olivier Romain†, Bram Vanderborght‡,
Romain Meeusen*, Bart Roelands* and Kevin De Pauw*

*Human Physiology and Sports Physiotherapy Research Group
Vrije Universiteit Brussel, Belgium
†Equipes Traitement de l'Information et Systèmes
CY Cergy Paris University, France
‡Robotics and MultiBody Mechanics Research Group
Vrije Universiteit Brussel and IMEC, Belgium

***Abstract*—Brain-computer interfaces can be used to operate devices by detecting a person's intention from their brain activity. Decoding motor imagery (MI) from electroencephalogram (EEG) signals is a commonly used approach for this purpose. To reliably identify MI from EEG signals, a sufficient number of sensors is usually required. However, a large number of sensors increases the computational cost of discriminating MI classes. Furthermore, consumer-grade devices that measure EEG signals often employ a reduced number of sensors compared to medical- or research-grade devices. In this experimental study, we investigate the tradeoff between accuracy and complexity when decoding MI from a restricted number of EEG sensors. For this purpose, several decoding pipelines were trained on EEG data using different subsets of electrode locations employing well-established decoding methods. We found that there is no significant difference (p=[0.18–0.91]) in average decoding accuracy when using fewer sensors. The largest loss in performance for a single individual was a reduction in mean decoding accuracy of 0.1 when using 8 out of 64 available sensors. Decoding MI from a limited number of sensors is therefore feasible, highlighting the potential of using commercial sensor devices for this purpose to reduce both monetary and computational costs.**

I. Introduction

Brain-computer interfaces (BCIs) allow users to operate devices with their thoughts. This type of interface could replace or improve interaction modalities such as speech recognition [1] or gesture control [2] among others. One of the main advantages of BCI is that the need to utter the words or perform the movement is removed [1]. Interacting with devices in this way could prove beneficial to people that suffer from a condition that affects speech or movement.

Thanks to recent technological advances, operating a device with an EEG-based BCI has become increasingly feasible [3], [4]. However, there are still several challenges that need to be addressed before BCI applications can move from the lab to the real world [5]. One such challenge is downscaling the amount of EEG sensors to reduce the computational cost of decoding and enable the use of consumer-grade portable EEG devices with small numbers of sensors (usually between 2 and 16) [6]. This would also allow a reduction in monetary costs for decoding hardware and EEG acquisition devices.

Hence, it is of interest to identify the minimal subset of sensors necessary to decode user intention reliably. Additionally, these sensors' optimal locations are also important for EEG decoding. Depending on the EEG modality used to generate commands, a specific subset of sensors will be necessary. One such modality is MI, which is the activity related to motor planning when executing a movement, but also occurs when imagining a movement.

Most research on reducing the number of sensors in EEG attempts to identify the optimal user-specific subset for MI decoding [7] or aims to use statistical methods to reduce the number of channels [8], [9]. This article aims to experimentally identify the minimal subset of electrodes and their optimal locations for MI classification. From existing literature on the functional regions of the brain, [10], the optimal locations would be expected around the motor cortex area of the brain. However, other types of brain responses, such as motor-onset visually evoked potentials [11] which are located in the occipital region of the brain, can also play a role in motor planning.

Since performing an exhaustive search of all possible sensor subsets would be computationally unfeasible, we decided to perform an empirical evaluation of decoding performance when using some specific sensor subsets, using common EEG decoding methods. The chosen sensor subsets were selected based on their usage in commercially available EEG devices or their involvement in motor functions of the brain.

II. Materials and Methods

A. Data Acquisition

The EEG data used in this study were acquired between august and October 2022. Ethical approval for the study was given by the ethical commission of human sciences of the Vrije Universiteit Brussel (ECHW_364.02). The dataset comprises 15 participants (14 male, 1 female) aged between 18 and 50 years. Each participant took part in 5 sessions on separate days. Each session consisted of multiple runs where a fixation cross was shown and movements were requested. There were two types of runs, depending on the session.

In calibration runs, participants had to either perform or imagine the requested movement. Whether to perform or imagine movement was orally communicated to the participant

before the start of a run. In feedback runs, a BCI decoding model was trained on previously acquired calibration data to give feedback. The feedback consisted of a textual message that told the participant if the decoded movement matches the requested movement. If there was a mismatch, the predicted movement was also shown. Feedback runs always used imagined movements.

The first 2 sessions were familiarization sessions where the participant was alternately tasked to perform and imagine movements without feedback. At the end of the second familiarization session, a first MI decoding model was trained on the data from the imagined movement run. This model was subsequently used in the first feedback run. The last 3 sessions each started with an imagined movement calibration run and three or more feedback runs. The decoding model for feedback was always trained on the data from the initial calibration run.

EEG data were acquired with a 64-channel LiveAmp (Brain Products GmbH) device at a sampling rate of 500 Hz, using active wet electrodes. Electrode locations follow the 10-20 system according to the 64-channel actiCap layout. The data link to the device was achieved over Bluetooth.

The stimulus presentation software was implemented in the Python programming language, using the Shady library [12]. The EEG signal and cue presentation timings were synchronized using the Labs Streaming Layer protocol[1]. The markers for movement initiation cues were recorded in a separate data stream. The synchronized data streams of EEG and marker streams were recorded in the XDF file format.

B. Data processing

EEG data were first pre-processed by following the standardized preprocessing offered by the PREP pipeline [13], [14]. The data were then filtered with a finite impulse response filter with a highpass frequency of 8 Hz and a lowpass frequency of 30 Hz as these frequencies contain most information related to MI [15]. The filter was designed as a one-pass, zero-phase, non-causal bandpass filter using a windowed time-domain design (firwin). The windowing method uses a Hamming window with 0.0194 passband ripple and 53 dB stopband attenuation. The lower transition bandwidth was 2.00 Hz and the upper transition bandwidth was 7.50 Hz, both with a -6 dB cutoff frequency. The filter length consisted of 825 samples resulting in a time window of 1.653 seconds. These design choices were based on the recommendations by [16].

The preprocessed data were split into epochs of 2 seconds before the movement initiation cue and 2 seconds after the cue and then resampled to 250 Hz. The epochs of individual runs of the same type and session for the same participant were merged to get individual datasets that were then used to evaluate the decoding pipeline.

Finally, the preprocessed data were used to train a decoding pipeline using Common Spatial Patterns (CSP, [17]) features and Linear Discriminant Analysis (LDA, [18]). This decoding pipeline was chosen for its low complexity and common usage [5] in MI decoding. The classification task consisted of distinguishing feet and right hand MI. For the CSP features, 4 components were used. The pipelines were evaluated by 5-fold cross-validation for each sensor subset. Mean cross-validation accuracies were compared with an independent sample t-test at a significance level of 0.05.

The considered sensor subsets were chosen based on existing datasets, the sensors used in commercial devices, and brain regions that are associated with motor control, such as the motor cortex located around the central brain areas [10]. Figure 1 shows the electrode positions for each subset according to the 10-20 system. The *Full* subset uses all 64 EEG channels, while the *Half* subset uses 32 channels by reducing the spatial resolution. The *BCI Comp* subset uses 21 of the 22 locations that are present in the BCI competition IV dataset 2a [19]. The FCz electrode was not available because the LiveAmp device uses it as the reference. The *OpenBCI 8* and *OpenBCI 16* subsets correspond to the default locations for the OpenBCI headset[2] in its 8-channel and 16-channel configurations respectively. Finally, the *Motor cortex* (MC) subset corresponds to the 24 locations associated with motor activity, and the *MC reduced* subset uses 9 of those locations.

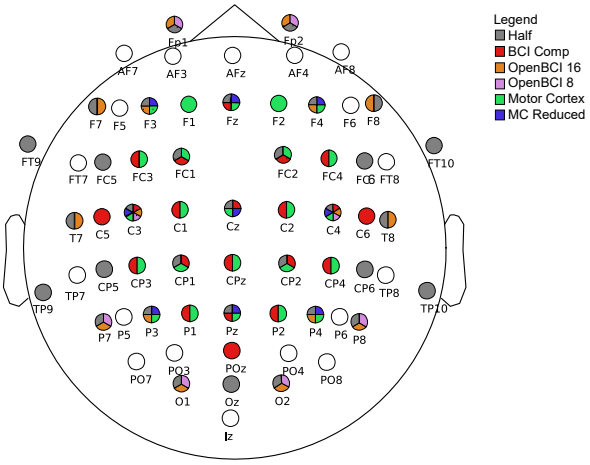

Fig. 1. Sensor locations of the different subsets. Empty circles indicate that the sensor location is not used in any subset.

Data were processed and analyzed using the MNE-Python software library for EEG analysis [20]. Machine learning methods that decode EEG were implemented with the Scikit-Learn library [21]. The libraries used for statistical analysis were Pandas [22] for data manipulation and SciPy [23] for statistical testing. Figures were generated with Seaborn [24].

III. Results

Table I gives an overview of the number of sensors, mean, standard deviation (std), minimum, and maximum cross-validation accuracy for each sensor subset over all participants.

Table I shows that there is great variability in the cross-validation results when using the full set of 64 channels, with

[1]https://labstreaminglayer.readthedocs.io/info/intro.html

[2]https://docs.openbci.com/AddOns/Headwear/MarkIV/

TABLE I
MEAN CROSS-VALIDATION ACCURACY RESULTS FOR EACH CONSIDERED SENSOR SUBSET.

	Full	Half	BCI Comp	OpenBCI 16	OpenBCI 8	Motor cortex	MC reduced
sensors	64	32	21	16	8	24	9
mean	0.67	0.67	0.67	0.66	0.65	0.66	0.65
std	0.15	0.16	0.15	0.15	0.15	0.16	0.15
min	0.31	0.31	0.34	0.23	0.34	0.27	0.35
max	1.00	1.00	1.00	0.98	0.93	1.00	0.94

a standard deviation of 0.15. For the full set of electrodes, the lowest accuracy was below random chance at 0.31, while the highest achieved accuracy was 1.00. The mean accuracy for the full set of sensors was 0.67. None of the differences in mean accuracy are statistically significant with p-values of 0.90 (half), 0.91 (BCI Comp), 0.74 (OpenBCI 16), 0.18 (OpenBCI 8), 0.52 (Motor cortex), and 0.25 (MC Reduced) when comparing to the full 64 sensor set.

Figure 2 visualizes the cross-validation results in a box-plot format to further investigate trends in the results.

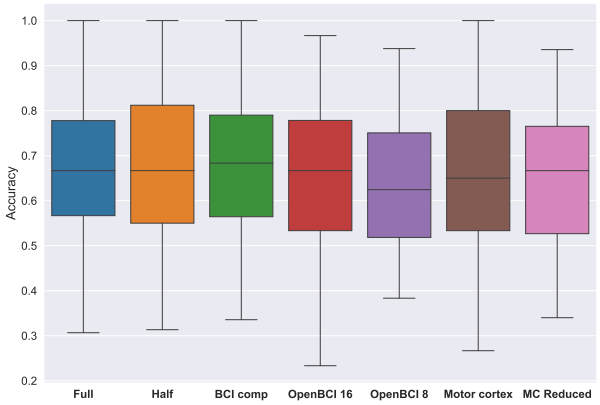

Fig. 2. Cross-validation accuracies for different sensor subsets.

From this figure, we can observe that the maximum accuracy is slightly lower for both OpenBCI sensor subsets and the MC reduced subset. For the other subsets, the maximum accuracy of 1.0 is retained. We can also observe that the minimum accuracy seems to increase for some sensor subsets, while it appears to decrease for others. The mean accuracy remains more stable, with the lowest being 0.65 for both *OpenBCI 8* and *MC reduced* subsets, which is the same for the median accuracy. However,

To investigate if this performance is maintained at the level of individual participants, we look at the decoding accuracies for both the participants where the highest and lowest mean decoding accuracy was achieved. These comparisons can be found in figures 3 and 4 respectively.

There are also no significant differences in mean accuracy for these particular participants, with p-values ranging between 0.55 and 0.84, and between 0.48 and 0.95, respectively. However, a reduced variance and an increase in minimum accuracy for specific sensor subsets can be observed. For example, for the BCI comp subset in figure 3, median accuracy is almost the same while minimum accuracy increases by more

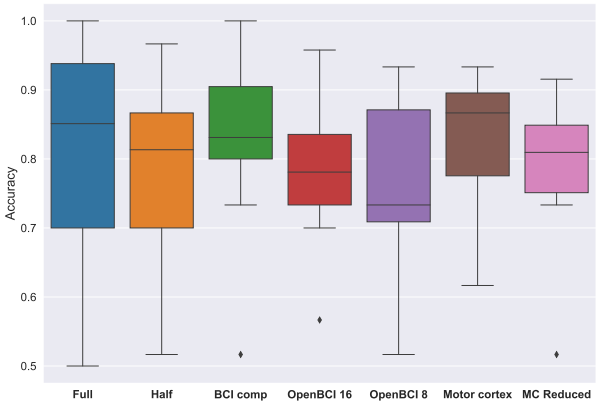

Fig. 3. Cross-validation accuracies for different sensor subsets for the participant with the best mean accuracy when using the full sensor set.

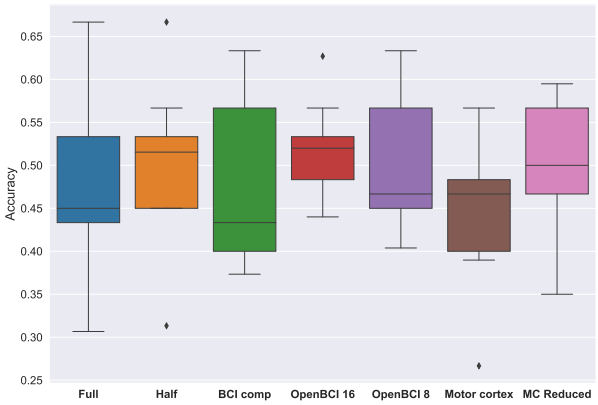

Fig. 4. Cross-validation accuracies for different sensor subsets for the participant with the worst mean accuracy when using the full sensor set.

than 0.2 (except for an outlier), and the boxplot boundaries show a reduced variance compared to the full set.

IV. Discussion

The goal of this research was to downscale the number of sensors that are necessary to decode imagined movements from EEG signals. To identify the minimal set of sensors that are necessary for this purpose and their optimal locations, an experimental study was performed. This study consisted of training a well-known decoding pipeline using different sensor subsets and comparing their cross-validation results.

From the results, we observe that the decoding accuracy does not significantly differ between the chosen sensor subsets. This highlights the feasibility of downscaling the number of sensors for BCI decoding purposes. It is noteworthy to mention that a large inter-individual variability exists, which is in line with current literature [25]. The obtained p-values for the subsets with fewer electrodes (i.e. OpenBCI 8 and MC Reduced) are smaller than those obtained for the larger subsets, which seems to indicate that there might be a threshold for the minimal number of sensors for MI decoding.

When comparing decoding performance at the participant level, the variance in decoding accuracy is reduced for certain

sensor subsets, indicating a more stable decoding performance. We can also observe that there is a difference in which specific subsets maintain (or in some cases improve) decoding performance for different individuals. This finding is also consistent with literature that aims to identify optimal user-specific sensor subsets [7].

An important finding of this study is that focusing solely on the motor cortex does not seem to be sufficient. Other areas, such as frontal and occipital areas of the brain seem to also contain information that is useful in differentiating MI. One possible explanation is that the model could learn to eliminate the noise in some sensors based on the activity in other locations. This is also consistent with the literature as, for example, the FP1 and FP2 locations are sometimes used solely to detect noise from frowning and eye movement [26]. For occipital areas, the motion-onset visually evoked potentials also appear to play a role in decoding MI [11].

We have shown that high-density EEG, typically defined as EEG setups with 64 sensors or more [27], is not essential for decoding MI and that this might even negatively affect decoding performance by introducing noise in the data. A relatively small number of electrodes could be used to decode imagined movement from EEG signals.

To determine the ideal number and location of sensors, future work should focus on additional sensor subsets and the effect of including or excluding specific sensor locations. Additionally, investigating inter-individual differences in decoding performance could also provide better insights into the sensor locations to include. By using more advanced methods that also learn a representation of the data, such as deep learning, an optimal set of sensors could also be identified in a data-driven way.

V. Conclusion

Decoding MI from EEG data is feasible with a relatively low number of sensors. Decoding accuracy does not significantly decrease when using fewer sensors. The largest loss in performance for an individual participant was observed for the smallest subset of 8 sensors with a difference of 0.1 in median accuracy, while the difference in maximum accuracy was lower at 0.05. On average over all participants, this decrease is not statistically significant (p=[0.18 - 0.91]). Therefore, using commercial EEG devices with a small number of sensors for BCI applications is feasible. However, more work is necessary to establish a standard optimal set of sensor locations by using more advanced decoding methods and investigating inter-individual differences in optimal sensor locations.

Acknowledgment

The authors would like to thank the people who participated in the data-gathering experiments and the students who assisted in the execution of these experiments.

References

[1] S.-H. Lee, M. Lee, and S.-W. Lee, "Neural Decoding of Imagined Speech and Visual Imagery as Intuitive Paradigms for BCI Communication," *IEEE Transactions on Neural Systems and Rehabilitation Engineering*, vol. 28, no. 12, pp. 2647–2659, Dec. 2020.

[2] T. I. Voznenko, E. V. Chepin, and G. A. Urvanov, "The Control System Based on Extended BCI for a Robotic Wheelchair," *Procedia Computer Science*, vol. 123, pp. 522–527, Jan. 2018.

[3] F. R. Willett *et al.*, "High-performance brain-to-text communication via handwriting," *Nature*, vol. 593, no. 7858, pp. 249–254, May 2021.

[4] Y. Liu, M. Habibnezhad, and H. Jebelli, "Brain-computer interface for hands-free teleoperation of construction robots," *Automation in Construction*, vol. 123, p. 103523, Mar. 2021.

[5] M. Rashid *et al.*, "Current Status, Challenges, and Possible Solutions of EEG-Based Brain-Computer Interface: A Comprehensive Review," *Frontiers in Neurorobotics*, vol. 14, 2020.

[6] R. Riedl *et al.*, "Consumer-Grade EEG Instruments: Insights on the Measurement Quality Based on a Literature Review and Implications for NeuroIS Research," in *Information Systems and Neuroscience*. Springer International Publishing, 2020, pp. 350–361.

[7] D. Gurve *et al.*, "Subject-specific EEG channel selection using non-negative matrix factorization for lower-limb motor imagery recognition," *Journal of Neural Engineering*, vol. 17, no. 2, p. 026029, Apr. 2020.

[8] S. Roy *et al.*, "Assessing impact of channel selection on decoding of motor and cognitive imagery from MEG data," *Journal of Neural Engineering*, vol. 17, no. 5, p. 056037, Oct. 2020.

[9] Y. Wang *et al.*, "EEG signal feature reduction and channel selection method in hand gesture recognition BCI system," in *2021 International Conference on Computer Engineering and Application (ICCEA)*, Jun. 2021, pp. 280–284.

[10] R. S. Snell, *Clinical Neuroanatomy*. Lippincott Williams & Wilkins, 2010.

[11] M. Kuba *et al.*, "Motion-onset VEPs: Characteristics, methods, and diagnostic use," *Vision Research*, vol. 47, no. 2, pp. 189–202, Jan. 2007.

[12] N. J. Hill *et al.*, "Shady: A software engine for real-time visual stimulus manipulation," *Journal of Neuroscience Methods*, vol. 320, pp. 79–86, May 2019.

[13] S. Appelhoff *et al.*, "PyPREP: A Python implementation of the preprocessing pipeline (PREP) for EEG data." Mar. 2022.

[14] N. Bigdely-Shamlo *et al.*, "The PREP pipeline: Standardized preprocessing for large-scale EEG analysis," *Frontiers in Neuroinformatics*, vol. 9, 2015.

[15] A. Singh *et al.*, "A comprehensive review on critical issues and possible solutions of motor imagery based electroencephalography brain-computer interface," *Sensors*, vol. 21, no. 6, pp. 1–35, 2021.

[16] A. Widmann, E. Schröger, and B. Maess, "Digital filter design for electrophysiological data – a practical approach," *Journal of Neuroscience Methods*, vol. 250, pp. 34–46, Jul. 2015.

[17] B. Blankertz *et al.*, "Optimizing Spatial filters for Robust EEG Single-Trial Analysis," *IEEE Signal Processing Magazine*, vol. 25, no. 1, pp. 41–56, 2008.

[18] G. J. McLachlan, *Discriminant Analysis and Statistical Pattern Recognition*. John Wiley & Sons, Inc., New York, 1992.

[19] M. Tangermann *et al.*, "Review of the BCI Competition IV," *Frontiers in Neuroscience*, vol. 6, 2012.

[20] A. Gramfort *et al.*, "MEG and EEG data analysis with MNE-Python," *Frontiers in Neuroscience*, vol. 7, 2013.

[21] F. Pedregosa *et al.*, "Scikit-learn: Machine Learning in Python," *Journal of Machine Learning Research*, vol. 12, no. 85, pp. 2825–2830, 2011.

[22] J. Reback *et al.*, "Pandas-dev/pandas: Pandas 1.0.3," Mar. 2020.

[23] P. Virtanen *et al.*, "SciPy 1.0: Fundamental algorithms for scientific computing in Python," *Nature Methods*, vol. 17, no. 3, pp. 261–272, Mar. 2020.

[24] M. L. Waskom, "Seaborn: Statistical data visualization," *Journal of Open Source Software*, vol. 6, no. 60, p. 3021, Apr. 2021.

[25] T. Nguyen *et al.*, "Classification of Multi-Class BCI Data by Common Spatial Pattern and Fuzzy System," *IEEE Access*, vol. 6, pp. 27 873–27 884, 2018.

[26] R. Bousseta *et al.*, "EEG Based Brain Computer Interface for Controlling a Robot Arm Movement Through Thought," *IRBM*, vol. 39, no. 2, pp. 129–135, Apr. 2018.

[27] S. Stoyell *et al.*, "High density EEG in current clinical practice and opportunities for the future," *Journal of clinical neurophysiology*, vol. 38, no. 2, pp. 112–123, Mar. 2021.